CALIBRATION OF A TEXTURE-BASED MODEL OF A GROUND-WATER FLOW SYSTEM, WESTERN SAN JOAQUIN VALLEY, CALIFORNIA

U.S. GEOLOGICAL SURVEY

Open-File Report 90-573

REGIONAL AQUIFER-SYSTEM ANALYSIS

Prepared in cooperation with the

SAN JOAQUIN VALLEY DRAINAGE PROGRAM

This report was prepared by the U.S. Geological Survey in cooperation with the San Joaquin Valley Drainage Program and as part of the Regional Aquifer-System Analysis (RASA) Program of the U.S. Geological Survey.

The San Joaquin Valley Drainage Program was established in mid-1984 and is a cooperative effort of the U.S. Bureau of Reclamation, U.S. Fish and Wildlife Service, U.S. Geological Survey, California Department of Fish and Game, and California Department of Water Resources. The purposes of the program are to investigate the problems associated with the drainage of agricultural lands in the San Joaquin Valley and to develop solutions to those problems. Consistent with these purposes, program objectives address the following key concerns: (1) public health, (2) surface- and ground-water resources, (3) agricultural productivity, and (4) fish and wildlife resources.

Inquiries concerning the San Joaquin Valley Drainage Program may be directed to:

San Joaquin Valley Drainage Program
Federal-State Interagency Study Team
2800 Cottage Way, Room W-2143
Sacramento, California 95825-1898

The RASA Program of the U.S. Geological Survey was started in 1978 following a congressional mandate to develop quantitative appraisals of the major ground-water systems of the United States. The RASA Program represents a systematic effort to study a number of the Nation's most important aquifer systems, which in aggregate underlie much of the country and which represent an important component of the Nation's total water supply. In general, the boundaries of these studies are identified by the hydrologic extent of each system, and accordingly transcend the political subdivisions to which investigations were often arbitrarily limited in the past. The broad objectives for each study are to assemble geologic, hydrologic, and geochemical information, to analyze and develop an understanding of the system, and to develop predictive capabilities that will contribute to the effective management of the system. The Central Valley RASA study, which focused on the hydrology and geochemistry of ground water in the Central Valley of California, began in 1979. Phase II of the Central Valley RASA began in 1984 and is in progress. The focus during this second phase is on more detailed study of the hydrology and geochemistry of ground water in the San Joaquin Valley, which is the southern half of the Central Valley.

CALIBRATION OF A TEXTURE-BASED MODEL OF A GROUND-WATER FLOW SYSTEM, WESTERN SAN JOAQUIN VALLEY, CALIFORNIA

By Steven P. Phillips *and* Kenneth Belitz

U.S. GEOLOGICAL SURVEY

Open-File Report 90-573

REGIONAL AQUIFER-SYSTEM ANALYSIS

Prepared in cooperation with the

SAN JOAQUIN VALLEY DRAINAGE PROGRAM

6439-59

Sacramento, California
1990

U.S. DEPARTMENT OF THE INTERIOR
MANUEL LUJAN, JR., *Secretary*

U.S. GEOLOGICAL SURVEY
Dallas L. Peck, *Director*

For sale by the Books and
Open-File Reports Section,
U.S. Geological Survey
Federal Center, Box 25425
Denver, CO 80225

For additional information write to:
District Chief
U.S. Geological Survey
Federal Building, Room W-2234
2800 Cottage Way
Sacramento, CA 95825

CONTENTS

FIGURES

TABLES

Conversion Factors

For readers who prefer to use the International System of Units (SI) rather than inch-pound units, the conversion factors for terms used in this report are listed below.

Multiply	By	To obtain
foot (ft)	0.3048	meter
foot per second (ft/s)	0.3048	meter per second
foot per year (ft/yr)	0.3048	meter per year
mile (mi)	1.609	kilometer
square mile (mi^2)	2.590	square kilometer

CALIBRATION OF A TEXTURE-BASED MODEL OF A GROUND-WATER FLOW SYSTEM, WESTERN SAN JOAQUIN VALLEY, CALIFORNIA

By Steven P. Phillips *and* Kenneth Belitz

ABSTRACT

The occurrence of selenium in agricultural drain water from the western San Joaquin Valley, California, has focused concern on the semiconfined ground-water flow system, which is underlain by the Corcoran Clay Member of the Tulare Formation. A two-step procedure is used to calibrate a preliminary model of the system for the purpose of determining the steady-state hydraulic properties. Horizontal and vertical hydraulic conductivities are modeled as functions of the percentage of coarse sediment, hydraulic conductivities of coarse-textured (K_{coarse}) and fine-textured (K_{fine}) end members, and averaging methods used to calculate equivalent hydraulic conductivities. The vertical conductivity of the Corcoran (K_{corc}) is an additional parameter to be evaluated.

In the first step of the calibration procedure, the model is run by systematically varying the following variables: (1) K_{coarse}/K_{fine}, (2) K_{coarse}/K_{corc}, and (3) choice of averaging methods in the horizontal and vertical directions. Root mean square error and bias values calculated from the model results are functions of these variables. These measures of error provide a means for evaluating model sensitivity and for selecting values of K_{coarse}, K_{fine}, and K_{corc} for use in the second step of the calibration procedure. In the second step, recharge rates are evaluated as functions of K_{coarse}, K_{corc}, and a combination of averaging methods. The associated K_{fine} values are selected so that the root mean square error is minimized on the basis of the results from the first step.

The results of the two-step procedure indicate that the spatial distribution of hydraulic conductivity that best produces the measured hydraulic head distribution is created through the use of arithmetic averaging in the horizontal direction and either geometric or harmonic averaging in the vertical. The equivalent hydraulic conductivities resulting from either combination of averaging methods compare favorably to field- and laboratory-based values.

INTRODUCTION

Recent studies in the Kesterson National Wildlife Refuge showed that many species of wildlife in the refuge have experienced adverse health conditions as a result of the influx of agricultural wastewaters, and in particular, the concentration of selenium (Se) in these waters (U.S. Bureau of Reclamation, 1984). The source area of the Se-bearing wastewaters was the central part of the western San Joaquin Valley, California (fig. 1). Subsurface drains were installed in this area during the early 1980's to control rising water levels, which posed a direct threat to the health of crop roots. The solute-bearing water pumped from these drains was transported by the San Luis Drain to the Kesterson

National Wildlife Refuge about 50 mi northwest of the drained area. In response to results of environmental impact studies, the plugging of the subsurface collection system that fed the San Luis Drain was begun in March 1985 and completed in April 1988 (Westlands Water District, 1989). Rising water levels and the associated increase in the area underlain by shallow ground water continue to be a management problem.

An analysis of regional ground-water flow in the source area is essential to the development of a solution to the problem of shallow ground water. The U.S. Geological Survey, as part of its Regional Aquifer-System Analysis Program and in cooperation with the San Joaquin Valley Drainage Program, is meeting this need by developing a numerical model of the ground-water flow system. This model will be used to test potential solutions to the problem, and thus aid in making management decisions. As a precursor to this model, a three-dimensional, texture-based, steady-state model of ground-water flow in the central part of the western San Joaquin Valley was developed for the purpose of determining the regional distribution of hydraulic conductivity.

PREVIOUS WORK

Various related studies have been done in or around the study area. The hydrology was studied extensively in the 1950's as agricultural development in the area increased, and the demand for water rose correspondingly (for example, Davis and Poland, 1957; Davis and others, 1959). Detailed discussions of the geology are included in reports by Miller and others (1971), Croft (1972), Hotchkiss (1972), and Page (1986). In addition, prior to the completion of the California Aqueduct, the U.S. Bureau of Reclamation (1965) prepared geologic maps and cross sections.

Recent studies of the ground-water flow system include those by Bull and Miller (1975) and Ireland and others (1984), who documented changes in the flow system resulting from agricultural development, including water-level declines and land subsidence. Belitz and Heimes (1990) provided a summary of previous work and used recently collected textural and water-level data to evaluate the character and evolution of the ground-water flow system in the study area from the early 1900's to 1986. Williamson (1982), Diamond and Williamson (1983), and Williamson and others (1989) developed a model of the ground-water flow system of the entire Central Valley. This model, though useful for purposes of comparison, is not of adequate scale to evaluate the ground-water flow system in the study area.

HYDROGEOLOGY

The study area is bordered on the west by the Coast Ranges and on the east by the valley trough, which is delineated by the San Joaquin River and the Fresno Slough. The study area is underlain by the Pleistocene Corcoran Clay Member of the Tulare Formation, which is a lacustrine deposit that divides the system vertically into a semiconfined zone (Davis and De Wiest, 1966) and a confined zone. The semiconfined zone is made up of Coast Range alluvium, Sierran sand, and flood-basin deposits (fig. 2). The confined zone consists of poorly consolidated flood plain, deltaic, alluvial-fan, and lacustrine deposits (Poland and others, 1975).

The Coast Range alluvium consists of poorly sorted alluvial-fan deposits derived from the Coast Ranges. These deposits, which comprise the majority of the materials above the Corcoran, consist of discontinuous lenses of fine- and coarse-grained materials. Although there are no distinct continuous aquifers or aquitards within the Coast Range alluvium, the term "semiconfined" is used to emphasize the cumulative effect of the vertically distributed fine-grained materials. Lithologically, the alluvial-fan deposits range from more than 80 percent sand and gravel in the fanhead regions to more than 80 percent silt and clay in the distal regions.

The Sierran sand, which interfingers with the Coast Range alluvium, is well-sorted, medium to coarse-grained micaceous sand derived from the Sierra Nevada. The uppermost expression of the interface between the Coast Range and Sierran deposits is close to the eastern boundary of the study area and is commonly overlain by flood-basin deposits.

Flood-basin deposits are derived from the Coast Ranges and the Sierra Nevada. These deposits are fine-grained, moderately to densely compacted clays that range in thickness from 5 to 35 ft (Belitz and Heimes, 1990).

Belitz and Heimes (1990) summarized the history of agricultural development in the study area. Agricultural development in the San Joaquin Valley, which began in the early 1900's, was sustained through ground-water withdrawal until 1967, when surface water was imported to the valley to decrease the dependence on ground water for irrigation. Heavy ground-water pumpage resulted in hydraulic head losses as much as several hundred feet in the confined zone, which in turn caused large-scale subsidence. The importation of surface water resulted in a decrease in ground-water withdrawal and a gradual recovery of hydraulic head in the confined zone.

Belitz and Heimes (1990) report that the dominant hydraulic controls on the semiconfined zone are application of irrigation water on the top of the system and historic pumpage from beneath the Corcoran and from deeper parts of the semiconfined zone. Consequently, there is a substantial downward head gradient in the study area. The vertical head gradient varies as a function of the texture of the deposits, which varies with geographic position. The fanheads and those areas dominated by Sierran sand have small vertical gradients (0.003 to 0.07) because of the high hydraulic conductivity of these deposits. The mid-fan and distal-fan areas are characterized by higher vertical gradients (0.07 to 0.32). Vertical gradients are large (0.08 to 1.1) beneath and near the California Aqueduct and in the fine-textured flood-basin deposits.

Horizontal hydraulic gradients are much smaller than the vertical gradients because the topographic relief in the study area is low. Locally, the topographic gradient reaches a maximum of 0.02 at the fanheads, and a minimum of 0.001 toward the valley trough. The hydraulic gradient seldom exceeds the topographic gradient.

MODELING APPROACH

A model of the study area was constructed using the U.S. Geological Survey's modular three-dimensional finite-difference ground-water flow model (McDonald and Harbaugh, 1984). The overall purpose of developing a model of the ground-water flow system in the central part of the western San Joaquin Valley is to create a tool that can be used to test potential solutions to the drainage problem. The primary goals of this phase of model development are to estimate the steady-state hydraulic properties of the system and to create a calibration strategy that can be used in future phases.

Governing Equation

The three-dimensional ground-water flow equation for steady-state flow in an anisotropic medium can be written as follows:

$$\frac{\partial}{\partial x}(K_H \frac{\partial h}{\partial x}) + \frac{\partial}{\partial y}(K_H \frac{\partial h}{\partial y}) + \frac{\partial}{\partial z}(K_v \frac{\partial h}{\partial z}) = 0 \qquad (1)$$

where

h = hydraulic head (L);
K_H = horizontal hydraulic conductivity (L/t);
K_v = vertical hydraulic conductivity (L/t); and
x,y,z = cartesian coordinates (L).

When the flow domain is divided vertically into multiple layers, the flow equation can be modified, as follows, to apply to each layer:

$$\frac{\partial}{\partial x}T\frac{\partial H_k}{\partial x}+\frac{\partial}{\partial y}T\frac{\partial H_k}{\partial y}+\lambda_{k+1}(H_{k+1}-H_k)+\lambda_{k-1}(H_{k-1}-H_k) = 0 \quad (2)$$

where

T = transmissivity (L^2/t) = $K_H b_H$,
where b_H = layer thickness (L);
λ = leakance (L/t) = K_v/b_v,
where b_v = thickness between layer midpoints (L);
k = layer number;

and

$$H = \frac{1}{z_2-z_1}\int_{z_1}^{z_2} dh = \text{vertically integrated hydraulic head,} \quad (3)$$

where

z_1 = elevation of bottom of aquifer (L); and
z_2 = elevation of top of aquifer (L).

Equation (2) is commonly applied in ground-water modeling investigations (for example, Jorgensen, 1975; Williamson and others, 1989) and is the form of equation used in the McDonald and Harbaugh (1984) model code.

Model Grid

The model grid is 20 columns by 36 rows, each grid cell measuring 1 mi on a side (fig. 1). In the vertical dimension, the grid is five layers deep (fig. 3), the upper two fixed in thickness at 20 and 30 ft. Layers 1 and 2 are fixed in order to have good control in the shallow part of the system because future phases of modeling will include the near-surface effects of evapotranspiration and discharge through shallow subsurface drains. The remaining thickness of deposits at a depth below 50 ft and above the Corcoran were divided arbitrarily into three layers, as there are no well-documented areally extensive aquifers or confining beds in the semiconfined zone: layers 3 to 5 are three-sixteenths, five-sixteenths, and one-half of the remaining thickness, respectively.

Boundary Conditions

The boundary conditions for the model are as closely related to natural hydrogeologic boundaries as possible. The upper boundary condition is the water table, which is modeled as specified head. The elevation of the water table was determined for each simulation period (1976, 1980, 1984) using an extensive water-level data base (Gronberg and others, 1989). The quantity of water-level data is such that for all years more than 50 percent of the model cells are within 1 mi of a well, and more than 95 percent of the cells are within 3 mi of a well.

The lower boundary condition must simulate the interaction between the semiconfined and confined zones. The model code (McDonald and Harbaugh, 1984) provides a general head boundary condition in which the flux out of (or into) a given cell is controlled by a conductance term and the head difference across the boundary:

$$Q = C(H_b - h_m) \tag{4}$$

where

Q = flow rate between a cell and the boundary (L^3/t);
C = conductance across the boundary (L^2/t);
H_b = head at the boundary (L); and
h_m = head in the model cell adjacent to the boundary (L).

When a general head boundary is used to model the interaction between two aquifers separated by a confining layer (for example, the Corcoran), the conductance term can be defined as follows:

$$C = \frac{AK}{b} \tag{5}$$

where

A = area of cell face adjacent to the boundary (L^2);
K = hydraulic conductivity of the confining layer (L/t); and
b = thickness of the confining layer (L).

The area of model cells and thickness of the Corcoran are known; therefore, the value required to solve for conductance is the hydraulic conductivity of the Corcoran (K_{corc}). K_{corc} was calibrated as described later in this paper.

The head difference across the Corcoran, which is the remaining term required to solve for the flux (eq. 4), is the difference between the heads in the lowermost layer in the semiconfined zone and the confined heads. Potentiometric heads in the confined zone were determined from contour maps prepared by Westlands Water District (written commun., 1987), California Department of Water Resources (written commun., 1987), and Ireland and others (1984).

Pumpage is not addressed explicitly in this model because of a lack of spatially accurate data. Overall, ground water accounts for between 5 and 20 percent of total applied water with more than one-half of the ground water pumped from the confined zone (Jo Ann Gronberg, U.S. Geological Survey, written commun., 1988). Pumpage from the confined zone is reflected in the confined potentiometric heads. Semiconfined zone pumpage was ignored in this model, which could result in substantial errors near pumping wells within the semiconfined zone.

The lateral boundary conditions are shown in figure 4. The western edge of the model is delineated by the contact between the consolidated marine deposits of the Coast Ranges and the unconsolidated alluvium to the east. The Coast Ranges act as a ground-water barrier, thus defining a no-flow boundary.

The eastern boundary follows the valley trough and is approximated by specified heads. The water table is well defined, and deeper heads are based on hydraulic heads measured in the Sierran sand near the eastern boundary, which vary minimally. Hydraulic heads between the water table and the Sierran deposits were estimated on the basis of typical vertical gradients in the distal-fan areas. The resulting specified-head boundary reflects a vertical gradient above the Sierran sand and no gradient within the Sierran sand, which is consistent with measured data.

The northern boundary is divided into western and eastern parts. The western part is a no-flow boundary defined by a flowline along the Little Panoche Creek fan. The eastern part of the northern edge, like the eastern boundary, was determined to be a specified-head boundary, which intersects the flowline at the northern limit of the study area. The southern boundary is no-flow based on a flowline which follows an axial path along the Cantua Creek fan.

TEXTURE-BASED ESTIMATION OF HYDRAULIC CONDUCTIVITY

Solution of the ground-water flow equation (eq. 2) requires specification of transmissivity and leakance. The thicknesses of the layers are known; therefore, the values required to solve for transmissivity and leakance are hydraulic conductivities in the horizontal and vertical directions. Values of horizontal and vertical hydraulic conductivity for the model were based on system-wide hydraulic conductivities of lithologic end members and an averaging method for interpolating between the end-member conductivities.

Two lithologic end members were identified in the semiconfined zone: coarse grained and fine grained. The percentage of coarse-grained materials is defined as texture and is mapped for each model cell. Coarse-grained material consists primarily of sand; clayey and silty sand; gravel; and clayey, silty, and sandy gravel. Fine-grained material is predominantly clay, silt, and sandy clay and silt. These criteria are essentially the same as those used by Page (1986).

The use of texture for the estimation of hydraulic parameters is common in ground-water modeling investigations (for example, Freeze and Cherry, 1979; Gutentag and others, 1984; Williamson and others, 1989). In addition, many textbooks define ranges of hydraulic conductivities on the basis of the grain size (texture) of the material (for example, Davis and De Wiest, 1966; Freeze and Cherry, 1979). In this investigation, texture is used through the application of functions which interpolate between the end-member hydraulic conductivities on the basis of a texture value for each model cell.

Given perfectly stratified material, equivalent horizontal hydraulic conductivity can be estimated using a weighted arithmetic mean between the end-member hydraulic conductivities, and equivalent vertical hydraulic conductivity can be estimated using a weighted harmonic mean. This approach commonly is used in ground-water modeling investigations. Deviations from this approach have been discussed by Gutjahr and others (1978) and Desbarats (1987). These studies suggest that in many cases a geometric average in the vertical direction is more appropriate than a harmonic average. The work of Desbarats (1987) and the fact that the study area does not contain perfectly stratified material provided the motivation for trying several different combinations of averaging methods in the horizontal and vertical directions.

Textural Data

The textural data used in this report were derived from several hundred drilling and geophysical logs as described by Laudon and Belitz (1989). Laudon and Belitz defined texture as the percentage of coarse-grained sediment present in a given subsurface depth interval as interpreted from a well log. Coarse-grained sediment is defined as consisting principally of sand, clayey and silty sand, gravel, and clayey, silty, and sandy gravel. Fine-grained sediment is defined as consisting principally of clay, silt, and sandy clay and silt. Textural values derived from the well logs were discretized into the model grid for each layer using a moving-average technique (Sampson, 1975). The quality of individual logs was determined by the frequency and detail of lithologic descriptions. The number of good to excellent quality well logs in layers 1 to 5 are 534, 383, 169, 136, and 98, respectively (Julie Laudon, U.S. Geological Survey, written commun., 1988). The wells from which these logs were taken provide good areal coverage of the model area in all layers, with relatively heavy concentrations along the California Aqueduct.

The textural values for all five layers range from about 0 to 99 percent coarse, and the system is predominantly fine grained. Seventy-five percent of the textural values in each model layer are less than 54 percent coarse, and the median values for layers 1 to 5 are 12, 26, 33, 36, and 28 percent coarse, respectively.

Equivalent Hydraulic Conductivity

In this study, each of the lithologic end members is assumed to have a unique value of hydraulic conductivity. Given the end-member conductivities and a textural value, an equivalent hydraulic conductivity can be calculated using various averaging methods. The three averaging methods considered in this investigation are arithmetic (A), geometric (G), and harmonic (H), and are defined as follows:

$$\text{A:}\quad K_{equiv} = (F_{coarse} \times K_{coarse}) + (F_{fine} \times K_{fine}) \tag{6a}$$

$$\text{G:}\quad K_{equiv} = \left[K_{coarse}^{F_{coarse}} \times F_{fine}^{K_{fine}} \right] \tag{6b}$$

$$\text{H:}\quad K_{equiv} = \frac{1}{\frac{F_{coarse}}{K_{coarse}} + \frac{F_{fine}}{K_{fine}}} \tag{6c}$$

where

K_{equiv} = equivalent hydraulic conductivity;
K_{coarse} = high end-member hydraulic conductivity;
K_{fine} = low end-member hydraulic conductivity;
F_{coarse} = coarse fraction of the texture;
F_{fine} = fine fraction of the texture; and
$F_{coarse} + F_{fine} = 1$.

Equivalent hydraulic conductivity based on the arithmetic mean is dominantly sensitive to the hydraulic conductivity and fraction of the coarse end member. In contrast, equivalent hydraulic conductivity based on the harmonic mean strongly weights the low-conductivity end member. The geometric mean falls between the two extremes acting much like the harmonic mean for fine materials and more like the arithmetic mean for the coarse end of the range.

Given the three averaging methods (A, G, and H) and the two directions (horizontal and vertical), nine combinations of averaging methods are possible. The fact that the horizontal hydraulic conductivity is greater than or equal to the vertical hydraulic conductivity in a horizontally layered system reduces the possible number of combinations to six (fig. 5).

For the sake of brevity, combinations of horizontal and vertical averaging methods are abbreviated by using the capital letters for each method, where the first letter identifies the horizontal averaging method and the second letter identifies the averaging method used in the vertical direction. For example, AG means that an arithmetic average was used in the horizontal direction, and a geometric average was used in the vertical direction.

Methods and Application

Model calibration is accomplished in two steps. In the first step, K_{coarse}, K_{fine}, and K_{corc} are varied systematically for each combination of averaging methods in the horizontal and vertical directions. Simulated heads are compared to measured heads, resulting in multiple combinations of parameters that best reproduce the measured head distribution. In the second step of calibration, the results from the head calibration are used to constrain the input parameters, and simulated fluxes are compared to estimated recharge rates. The second step, which results in unique sets of parameters and averaging methods, is discussed after the results of the first step.

In the head calibration, simulated head values were compared to water levels from 41 wells (fig. 6) screened below the water table and above the Corcoran. The length of the screened intervals ranges from 20 to 270 ft and typically is less than 100 ft. The screened interval of each of the 41 wells was compared to the depths of the model layers at the geographic location of the well. The layer with the midpoint closest to the midpoint of the screened interval was selected as the model cell to be compared to the measured value.

Three unknowns must be identified to calibrate the steady-state model: K_{coarse}, K_{fine}, and K_{corc}. The three unknowns were reduced to two independent variables for the head calibration:

$$K' = K_{coarse}/K_{corc}$$
$$K'' = K_{coarse}/K_{fine}$$

Various statistical values can be calculated from the results of a model run for a given (K′, K″). These values can be described as dependent variables. The two dependent variables selected for the first step of the calibration procedure are the root mean square error and the bias, which are defined as follows:

$$\text{– root mean square error: } G_{rmsq}(K',K'') = \frac{\sqrt{\sum_{i=1}^{n} [h_{obs(i)} - h_{sim(i)}]^2}}{n} \quad (7a)$$

$$\text{– bias: } G_{bias}(K',K'') = \sum_{i=1}^{n} [h_{obs(i)} - h_{sim(i)}] \quad (7b)$$

where

n = number of measured values;
h_{obs} = head at an observation point; and
h_{sim} = head in the model cell representing the corresponding observation point.

The root mean square error is a relative measure of the error associated with the difference between simulated and measured heads. Positive or negative differences in head have equal effects on the calculations. System-wide tendencies toward positive or negative head differences are reflected in the bias value.

Systematically varying K′ and K″ over a range of values and running the model for each pair yields a set of root mean square error and bias results for a given combination of horizontal and vertical averaging methods. The set of results is then arranged into the form of a matrix. The solution matrices for each combination of averaging methods then can be compared. Fortran programs were developed, which accomplish the task of systematically changing the two independent variables and compiling the results (Phillips, 1988).

The model results can be displayed using what we define as "maps" (fig. 7). These maps are essentially 3-dimensional graphs with K′ on the horizontal axis and K" on the vertical axis. Plotting the root mean square error or bias associated with each (K′, K″) or each plus (+) symbol in figure 7 results in the definition of a 3-dimensional surface. These surfaces can be contoured to show patterns from which inferences can be drawn concerning the sensitivity of the system and the viability of the designated combination of averaging methods. In summary, each point on the map in figure 7 represents a statistical result (for example, root mean square error or bias) from a model run for a given (K′, K″) and combination of horizontal and vertical averaging methods.

Preliminary Results

Contoured root mean square error and bias maps for six combinations of horizontal and vertical averaging methods for 1984 are shown in figures 8a and 8b. These maps show that the distributions of root mean square error and bias are heavily dependent on the relative values of K_{corc} and K_{fine}.

The points in the upper right-hand corners of the maps in figure 8a all have similar values and define gently sloping plateaus. The combination of a low K_{corc} and a high K_{fine} prohibits the establishment of a vertical gradient in the semiconfined zone, and the water table completely controls the system. The lower left-hand corner of the maps show the opposite effect--a high K_{corc} and a low K_{fine} allows the system to drain easily from the bottom. This results in large vertical gradients and correspondingly large errors.

Note that the diagonals from the upper left to the lower right consist of relatively constant values, with the exception of the AA case. In addition to forming lines of relatively constant values, the diagonals also define the axis of a valley in the root mean square error surface. The orientation of this axis, or line of minimum root mean square error, indicates that the Corcoran is 1 to 1.5 orders of magnitude lower in conductivity than the semiconfined clay.

The contoured bias maps show patterns similar to the root mean square error (fig. 8b). Close inspection, however, shows that the lines of minimum root mean square error and zero bias do not coincide although they are nearly parallel. The negative bias values associated with the minimum root mean square error indicate that the simulated head generally is higher than the measured head when the root mean square error is minimized.

The maps in figures 8a and 8b show that there are many ways to achieve the same result. No single combination of averaging methods produces a superior distribution of hydraulic conductivity using hydraulic head as the sole criteria; therefore, the model also was calibrated against flux. The results of the first step of calibration were used to constrain the parameters for the flux calibration.

FLUX-CONSTRAINED CALIBRATION

Methods and Application

In the second step of the calibration procedure, simulated and estimated recharge rates were compared. Simulated recharge rates in selected parts of the study area were estimated as functions of K_{coarse} and K_{corc} for the various combinations of averaging methods. Recharge in these areas was estimated from water budget and irrigation efficiency data compiled by G.S. Hoffman and Byron Steinert (USDA-Agricultural Research Service, written commun., 1987).

Hoffman and Steinert compiled water budget and irrigation efficiency data in four separate 5 to 6 mi^2 areas, two in the drained area (downslope) and two upslope from the drained area (fig. 6). The irrigation efficiency reflects the portion of irrigation water that is used by plants. The remaining water is assumed to get past crop roots and becomes recharge to the ground-water system. The average estimated downslope recharge from the two downslope areas studied is 0.52 ft/yr; the average estimated upslope recharge is 1.57 ft/yr; and the ratio of upslope to downslope recharge is 3.0.

The model equivalent of recharge was defined as the flux through the bottom of the cell containing the water table. The average fluxes from model cells within the same four areas studied by Hoffman and Steinert were compared to the estimated recharge. The upslope flux, downslope flux, and flux ratio were mapped as functions of K_{coarse} and K_{corc}. For each combination of K_{coarse} and K_{corc}, K_{fine} was selected so that the root mean square error from the first step of calibration was minimized (see fig. 9 for explanation). The resulting maps of flux and flux ratio then were compared to estimated recharge and recharge ratio.

The ranges of K_{coarse} and K_{corc} over which the model was run were selected using values reported by previous workers. The prominent coarse-grained lithology in the study area is sand, and data from Johnson and others (1968) show that the hydraulic conductivity of sand in and around the study area ranges from about 3×10^{-5} to 3×10^{-3} ft/s. The results from the Central Valley study (Williamson and others, 1989) show that the hydraulic conductivity of the Corcoran ranges from 3×10^{-9} to 2×10^{-8} ft/s.

Results

The model was run systematically over the ranges of K_{coarse} and K_{corc} indicated by previous workers. Maps of upslope flux, downslope flux, and flux ratio were produced for the following combinations of horizontal and vertical averaging methods: AG, AH, GG, GH, and HH. The AA case was not included because the line of minimum root mean square error for the AA case is nearly vertical, and one cannot pick a value of K_{fine} that minimizes the root mean square error for any reasonable combination of K_{coarse} and K_{corc}.

Analysis of the flux maps showed that some combinations of averaging methods are incapable of simultaneously simulating the estimated upslope and downslope recharge within the specified K_{coarse} and K_{corc} ranges. For the GG, GH, and HH cases, the ratio of upslope to downslope flux is a constant value of 1.34, which does not compare well with the estimated value of 3.0. The AG and AH cases, however, are capable of simultaneously simulating the estimated upslope and downslope recharge. This indicates that an arithmetic average in the horizontal direction is required in order to produce the estimated recharge. This requirement for relatively high horizontal flow suggests that sand bodies in the Coast Range alluvium are laterally connected across cell boundaries.

The AG and AH maps of upslope and downslope flux indicate that there are unique solutions where the correct upslope and downslope fluxes coexist. Figure 10 shows the upslope and downslope fluxes for the AG and AH cases over a grid with one-eighth order of magnitude spacing surrounding these solutions. For the AG case, figure 10 indicates that the model reproduces estimated upslope and

downslope fluxes if K_{coarse} is 3.5×10^{-4} ft/s and K_{corc} is 1.2×10^{-8} ft/s; the corresponding K_{fine} is 1.2×10^{-7} ft/s. For the AH case, figure 10 indicates K_{coarse} is 6.3×10^{-4} ft/s, and K_{corc} is 8.3×10^{-9} ft/s with a corresponding K_{fine} of 5.4×10^{-7} ft/s.

The K_{corc} values which optimize the model (1.2×10^{-8} ft/s and 8.3×10^{-9} ft/s for the AG and AH cases, respectively) compare favorably with the results from the Central Valley study (Williamson and others, 1989). As discussed earlier, the K_{corc} values from the Central Valley study indicate a range of 3×10^{-9} to 2×10^{-8} ft/s. The AG and AH K_{corc} values fall within this range.

The K_{corc} values indicated by the model and by the Central Valley study are higher than the values reported in the literature. Permeameter tests for the Corcoran range from 3×10^{-10} to 7.8×10^{-9} ft/s, and consolidation tests range from 3.7×10^{-11} to 6.0×10^{-11} ft/s (Davis and others, 1964).

Williamson and others (1989) proposed an explanation for the discrepancy between model results and laboratory measurements. They concluded that wells drilled through the Corcoran could provide pathways for enough flow to raise the overall K_{corc} and that five wells per township could account for the increased conductance. Preliminary evaluation of the Survey's data base indicates that about 10 wells per township are screened above and below the Corcoran (Jo Ann Gronberg, U.S. Geological Survey, written commun., 1988).

Slug tests were done in 25 wells drilled by the U.S. Geological Survey in order to independently assess the hydraulic conductivity of coarse-grained materials. Each well has a 5- or 10-foot screen and sand pack, and the screened interval is exclusively within sandy materials. The holes were grouted from the sand pack to the land surface. The slug test data were interpreted using the method of Cooper and others (1967) as expanded by Papadopulos and others (1973). A summary of the results and some statistical analyses are presented in table 1. The average horizontal hydraulic conductivity for all 25 wells was 6.3×10^{-4} ft/s, which compares favorably with the two values of K_{coarse} for the AG and AH cases (3.5×10^{-4} and 6.3×10^{-4} ft/s, respectively). The median of the 25 wells also is within the range with a value of 4.2×10^{-4} ft/s.

A comparison of the optimum K_{fine} values (1.2×10^{-7} and 5.4×10^{-7} ft/s for the AG and AH cases, respectively) with laboratory-measured core values in and around the study area (table 2) suggests that the fine end member controlling vertical flow is between a sandy silt and a sandy silty clay. The semiconfined zone is known to contain significant deposits of clay. In a layered system, these low-permeability deposits would be the limiting factor controlling vertical flow. Because K_{fine} is greater than the hydraulic conductivity of clay, one may conclude that clay bodies in the semiconfined zone probably are not laterally extensive. In contrast, because K_{coarse} is close to the hydraulic conductivity of sand in table 2, one may conclude that sand bodies in the semiconfined zone probably are laterally extensive over distances greater than one model cell (1 mi).

The model results indicate that arithmetic averaging is required in the horizontal direction. Consequently, the range in equivalent horizontal hydraulic conductivity for the AG and AH cases is relatively small. The results also indicate that the geometric and harmonic averages work in the vertical direction. Because the geometric average is more sensitive than the harmonic average to textural variations, the ranges of equivalent vertical hydraulic conductivity differ for the AG and AH cases. Fifty percent of the model cells contain 18- to 52-percent coarse-grained materials. In the AH case, anisotropy, which is defined as the ratio of horizontal to vertical hydraulic conductivity, ranges from 100:1 to 500:1 for this range of texture. The anisotropy for the AG case for the same textural values ranges from 8:1 to 360:1.

TESTING THE STEADY-STATE ASSUMPTION

One potential error that could have a significant effect on the validity of the results from this phase of modeling is the assumption that the system can be represented by a steady-state simulation. The steady-state assumption was checked in two ways: (1) the model was run for three separate time periods and (2) the confined heads were altered, assessing potential error from a transient response between changes in confined and semiconfined heads.

Three time periods were selected for the purpose of checking the variability of model results over time. If the contoured maps from each time period proved similar, this would indicate that the system can be represented by a steady-state simulation within the range of time periods. The years 1976, 1980, and 1984 were selected because of the availability of data in those years and the fact that water levels showed a large system-wide recovery in the semiconfined and confined zones during that time range. Any variations in precipitation or irrigation between these years are negligible compared to the system-wide recovery from historical pumping.

Figure 11 shows the results from one combination of averaging methods for all three time periods. Inspection of the maps for each time period shows that the patterns defined by the contours remain fairly steady over the time range, and the magnitude of error decreases over time. The results from all other combinations of averaging methods show similar trends.

At least three explanations are possible for the decreasing magnitude of error over time. First, the smaller amount of available data in the earlier time periods may have caused a decrease in the accuracy of the water-table maps. Second, pumpage in the semiconfined zone may have decreased over time with the increased availability of surface water. Third, there may be a significant lag between head changes in the confined zone and the response in the semiconfined zone to those changes. Any error caused by this lag would be maximized when the rate of change in the confined heads is at its greatest. In 1976, confined heads were changing much more rapidly than in 1984. The preceding arguments indicate that using 1984 values for a steady-state solution minimizes the errors associated with the steady-state assumption.

Using the 1984 simulation period, the second test of the steady-state assumption was to replace the 1984 confined heads with those from 1967, which represent the historically lowest confined heads. The results from this simulation reflect the maximum possible lag between head changes in the confined and semiconfined zones. Figure 12 shows the results from the same combination of averaging methods (AG) as shown in figure 11. Inspection shows that the values are all shifted by less than one-half an order of magnitude to the right (decreasing K_{corc}). Because this shift is minimal and because the patterns defined by the contours remain identical, the error associated with a lag between head changes in the confined and semiconfined zones can be considered insignificant.

DISCUSSION OF ERRORS

In each step in the modeling process, there is the potential for introducing error. The errors associated with the optimum AG and AH solutions are essentially identical, with a root mean square error of about 19 ft and an average bias of about -5. Possible sources of error include the following: (1) specification of boundary conditions, (2) estimation of texture, (3) use of wells as calibration points, and (4) use of recharge as a calibration parameter. Steps can be taken in future phases of model development to minimize errors from these sources.

The upper and lower boundary conditions control, to a large extent, the hydraulic head in the system. The results from the first phase of calibration showed that the water table had much more influence than the confined heads on the head distribution in the semiconfined zone. Reduction of error in future phases of modeling could be accomplished by more accurate mapping of the water table.

Neglecting pumpage from the semiconfined zone can cause large errors in those areas that are strongly affected by local pumping. Figure 13 is a pair of histograms showing the distribution of errors for the AG and AH solutions. Although most of the simulated heads are within 5 ft of the measured heads, there are a significant number of large errors, particularly negative errors. Several of the large negative values are associated with wells screened in the Sierran sand, which have water levels significantly lower than those in nearby wells and probably are affected by local pumping. Explicit treatment of semiconfined zone pumpage should improve the model results.

The distribution of the textural data and the analysis of that distribution are other possible sources of error. Textural distribution was estimated separately for each of the five model layers, thus ignoring data points in adjacent layers. The estimated textural distribution could be improved in future phases of model development through the use of statistical methods which take into account the vertical as well as the horizontal distribution of data. Such an approach would be especially helpful in the deeper layers where the data density is lowest.

The assumption that there are two lithologic end members in the semiconfined zone may contribute to model error. Analysis of slug test results indicates that Sierran sand is, on the average, three times more permeable than the sand in the Coast Range alluvium. With minor modifications, the calibration strategy presented in this paper could accommodate this additional end member.

The use of wells as calibration points introduces additional error. The comparison between a simulated value at the midpoint of a model cell and the head at the midpoint of the screened interval introduces error proportional to the vertical gradient over the distance between the two midpoints. Also, many of the wells used were not intended to be observation wells; some of these wells have large screened intervals and/or gravel packs over the entire length of the casing. Therefore, comparison of well data and model cell head in future phases of modeling should account for (1) the proximity of the screened interval to the midpoint of a model layer and (2) the way the well was constructed.

A major problem in evaluating the ground-water flow system in the central part of the western San Joaquin Valley is the difficulty in estimating the areal distribution of recharge. An alternative to calibrating the model against the flux across the water table is calibration against other fluxes in the system. These include the fluxes across the eastern and/or lower boundaries. To improve the model in this respect, a more accurate estimation of the water budget will be required.

SUMMARY AND CONCLUSIONS

A three-dimensional steady-state model of the ground-water flow system in the central part of the western San Joaquin Valley, California, was developed for the purpose of determining the regional distribution of transmissivity and leakance. Transmissivity and leakance values for individual model cells were determined as a function of the percentage of coarse materials in each model cell, system-wide end-member hydraulic conductivities (K_{coarse} and K_{fine}), and methods for interpolating between the end members. Three methods were used for the interpolation: the arithmetic, geometric, and harmonic averages. The hydraulic conductivity of the Corcoran (K_{corc}) was an additional unknown.

The calibration procedure took place in two steps. In the first step, simulated head was compared to measured head. Root mean square error and bias were mapped as functions of K_{coarse}/K_{corc} and K_{coarse}/K_{fine}. Contouring of these maps revealed valley-shaped structures that defined a line of minimum error for each map. A conclusion reached during the head calibration was that K_{corc} is 1 to 1.5 orders of magnitude lower than K_{fine}.

In the second step of the calibration procedure, flux across the water table was mapped as a function of K_{coarse} and K_{corc}. Using the results of the first step, K_{fine} was selected so that the root mean square error was minimized. A conclusion reached during the flux calibration was that a significant component of horizontal flow is required to reproduce the estimated recharge. The arithmetic average was

the only method that produced equivalent horizontal hydraulic conductivities large enough to achieve the required flow rates. The requirement of an arithmetic average suggests that the sand in the Coast Range alluvium is connected horizontally over distances greater than one grid cell (more than 1 mi).

The results from the flux calibration also indicate that the geometric and harmonic averaging methods work in the vertical direction and that the arithmetic method does not. The resulting fine-grained end member controlling vertical flow ranges in composition from a sandy silt to a silty sandy clay. One may deduce from this result that, on the average, clay beds are not laterally continuous at scales larger than model cells.

In general, the model reproduces measured and estimated data reasonably well. Simulated heads are accurate to within an average of about 13 ft of the measured values and simulated flux can match estimated recharge. In addition, K_{coarse} and K_{corc} compare favorably to values determined from field testing and from previous studies.

Analysis of the model results showed several potential ways to improve the solution in future phases of model development:

(1) construction of a more accurate map of the water table;
(2) separation of semiconfined zone pumpage from the lower boundary condition;
(3) re-discretization of the textural data, taking advantage of the vertical as well as the horizontal distribution of data;
(4) use of a separate K_{coarse} for the Sierran and Coast Range deposits;
(5) careful selection of observation wells used as calibration points; and
(6) calibration of the model against fluxes across the eastern and/or lower boundaries. This requires a more accurate and extensive estimate of the water budget.

The two-step calibration procedure, which was developed for this first phase of modeling, is a valuable tool for the purposes of calibration and sensitivity analysis. The procedure was designed to be flexible and should prove useful in future phases of this modeling effort and in other applications.

REFERENCES CITED

Belitz, Kenneth, and Heimes, F.J., 1990, Character and evolution of the ground-water flow system in the central part of the western San Joaquin Valley, California: U.S. Geological Survey Water-Supply Paper 2348, p.

Bull, W.B., and Miller, R.E., 1975, Land subsidence due to ground-water withdrawal in the Los Banos-Kettleman City area, California, Part I. Changes in the hydrologic environment conducive to subsidence: U.S. Geological Survey Professional Paper 437-E, 71 p.

Cooper, H.H., Bredehoeft, J.D., and Papadopulos, I.S., 1967, Response of a finite diameter well to an instantaneous charge of water: Water Resources Research, v. 3, no. 1, p. 263-269.

Croft, M.G, 1972, Subsurface geology of the Late Quaternary water-bearing deposits of the southern part of the San Joaquin Valley, California: U.S. Geological Survey Water-Supply Paper 1999-H, 29 p.

Davis, G.H., and Poland, J.F., 1957, Ground-water conditions in the Mendota-Huron area, Fresno and Kings Counties, California: U.S. Geological Survey Water-Supply Paper 1360-G, 588 p.

Davis, G.H., Green, J.H., Olmsted, F.H., and Brown, D.W., 1959, Ground-water conditions and storage capacity in the San Joaquin Valley, California: U.S. Geological Survey Water-Supply Paper 1469, 287 p.

Davis, G.H., Lofgren, B.E., and Mack, S., 1964, Use of ground-water reservoirs for storage of surface water in the San Joaquin Valley, California: U.S. Geological Survey Water-Supply Paper 1618, 125 p.

Davis, S.N., and De Wiest, R.J.M., 1966, Hydrogeology: John Wiley and Sons, New York, 463 p.
Desbarats, A.J., 1987, Numerical estimation of effective permeability in sand-shale formations: Water Resources Research, v. 23, no. 2, p. 273-286.
Diamond, J., and Williamson, A.K., 1983, A summary of ground-water pumpage in the Central Valley, California, 1961-77: U.S. Geological Survey Water-Resources Investigations Report 83-4037, 70 p.
Freeze, R.A., and Cherry, J.A., 1979, Groundwater: New Jersey, Prentice-Hall, 604 p.
Gronberg, J.M., Belitz, Kenneth, and Phillips, S.P., 1989, Description of wells in the western part of San Joaquin Valley, California: U.S. Geological Survey Water-Resources Investigations Report 89-4158, 51 p.
Gutentag, E.D., Heimes, F.J., Kroth, N.C., Luckey, R.R., and Weeks, J.B., 1984, Geohydrology of the high plains aquifer in parts of Colorado, Kansas, Nebraska, New Mexico, Oklahoma, South Dakota, Texas, and Wyoming: U.S. Geological Survey Professional Paper 1400-B, 63 p.
Gutjahr, A.L., Gelhar, L.W., Bakr, A.A., and MacMillan, J.R., 1978, Stochastic analysis of spatial variability in subsurface flows 2. Evaluation and application: Water Resources Research, v. 15, no. 5, p. 953-959.
Hotchkiss, W.R., 1972, Generalized subsurface geology of the water-bearing deposits, northern San Joaquin Valley, California: U.S. Geological Survey Open-File Report 73-119, 18 p.
Ireland, R.L., Poland, J.F., and Riley, F.S., 1984, Land subsidence in the San Joaquin Valley through 1980: U.S. Geological Survey Professional Paper 437-I, 93 p.
Johnson, A.I., Moston, R.P., and Morris, D.A., 1968, Physical and hydrologic properties of water-bearing deposits in subsiding areas in central California: U.S. Geological Survey Professional Paper 497-A, 71 p.
Jorgensen, D.G., 1975, Analog model studies of ground-water hydrology in the Houston district, Texas: Texas Water Development Board Report 190, 84 p.
Laudon, Julie, and Belitz, Kenneth, 1989, Texture and depositional history of near-surface alluvial deposits in the central part of the western San Joaquin Valley, California: U.S. Geological Survey Open-File Report 89-235, 19 p.
McDonald, M.G., and Harbaugh, A.W., 1984, A modular three-dimensional finite-difference ground-water flow model: U.S. Geological Survey Open-File Report 83-875, 526 p.
Miller, R.E., Green, J.H., and Davis, G.H., 1971, Geology of the compacting deposits in the Los Banos-Kettleman City Subsidence area, California: U.S. Geological Survey Professional Paper 497-E, 46 p.
Page, R.W., 1986, Geology of the fresh ground-water basin of the Central Valley, California, with texture maps and sections: U.S. Geological Survey Professional Paper 1401-C, 54 p.
Papadopulos, I.S., Bredehoeft, J.D., and Cooper, H.H., Jr., 1973, On the analysis of "slug test" data: Water Resources Research, v. 9, no. 4, p. 1087-1089.
Phillips, S.P, 1988, Calibration of a texture-based simulation of the ground-water flow system in the western San Joaquin Valley, California: Unpublished Masters thesis, San Jose State University, 142 p.
Sampson, R.J., 1975, Surface II graphics system: Series on Spatial Analysis, Kansas Geological Survey, 240 p.
U.S. Bureau of Reclamation, 1965, San Luis Unit, Central Valley Project, California. Ground-water conditions and potential pumping resources above the Corcoran Clay. An addendum to the "Ground-water geology and resources definite Plan Appendix 1963: U.S. Bureau of Reclamation.
U.S. Bureau of Reclamation, 1984, Kesterson Reservoir and waterfowl: Information Bulletin 2, 11 p.
Westlands Water District, 1989, Water supply replacement project: Draft Environmental Impact Report/Statement, 376 p.
Williamson, A.K., 1982, Evapotranspiration of applied water, Central Valley, California, 1957-1978: U.S. Geological Survey Water-Resources Investigation 81-45, 56 p.
Williamson, A.K., Prudic, D.E., and Swain, L.A., 1989, Ground-water flow in the Central Valley, California: U.S. Geological Survey Professional Paper 1401-D, 127 p.

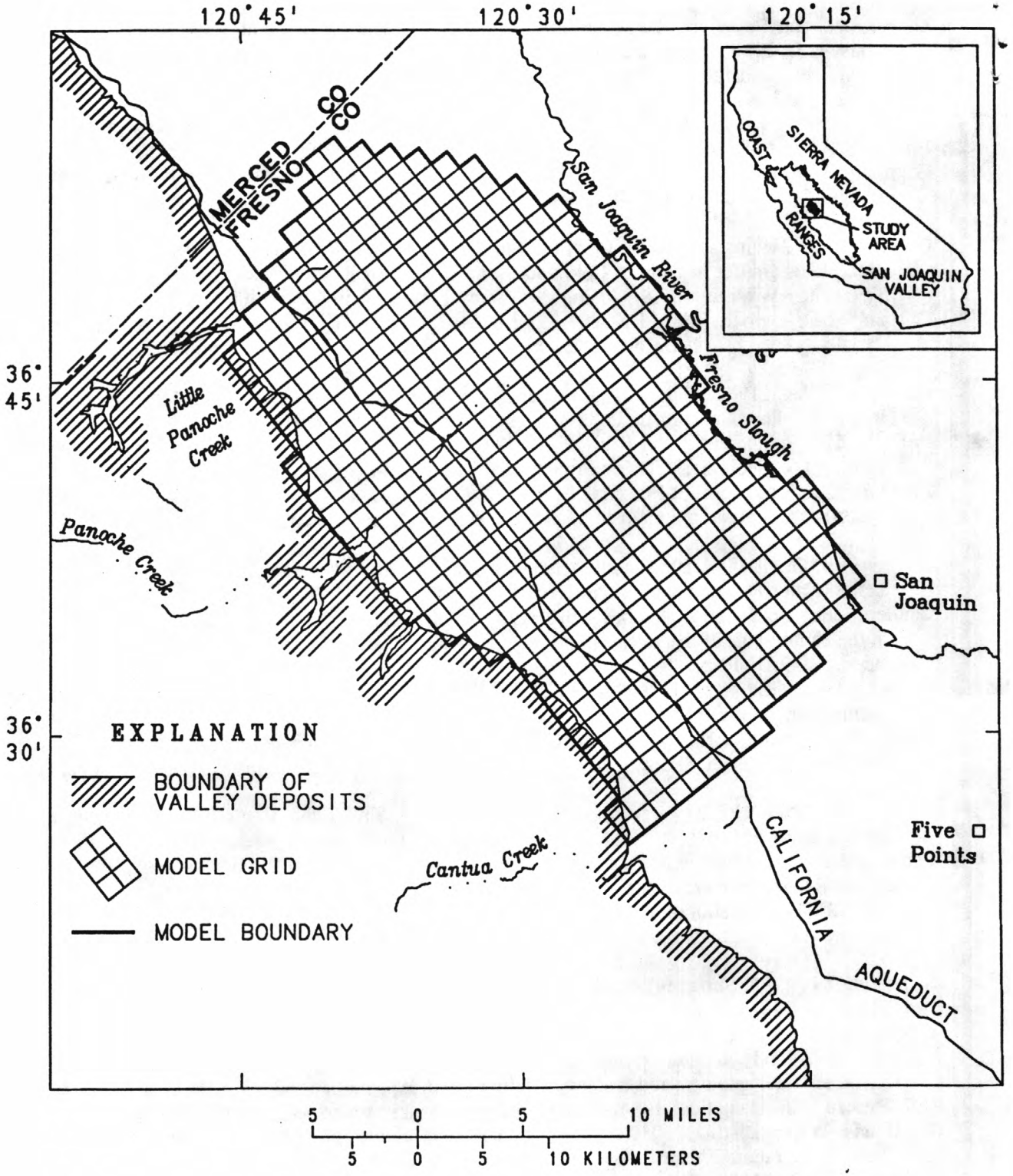

Figure 1.—Location of study area and configuration of model grid.

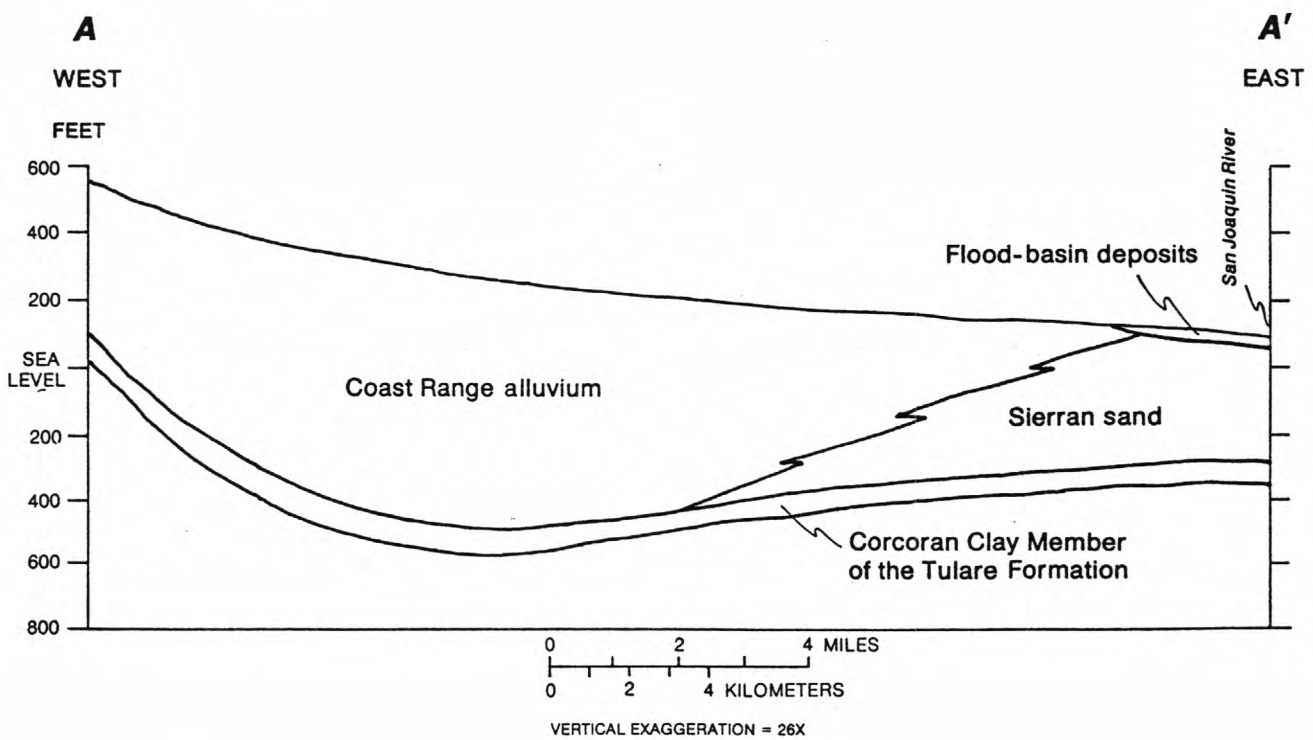

Figure 2. Generalized geohydrologic section of the semiconfined zone perpendicular to the axis of the San Joaquin Valley.

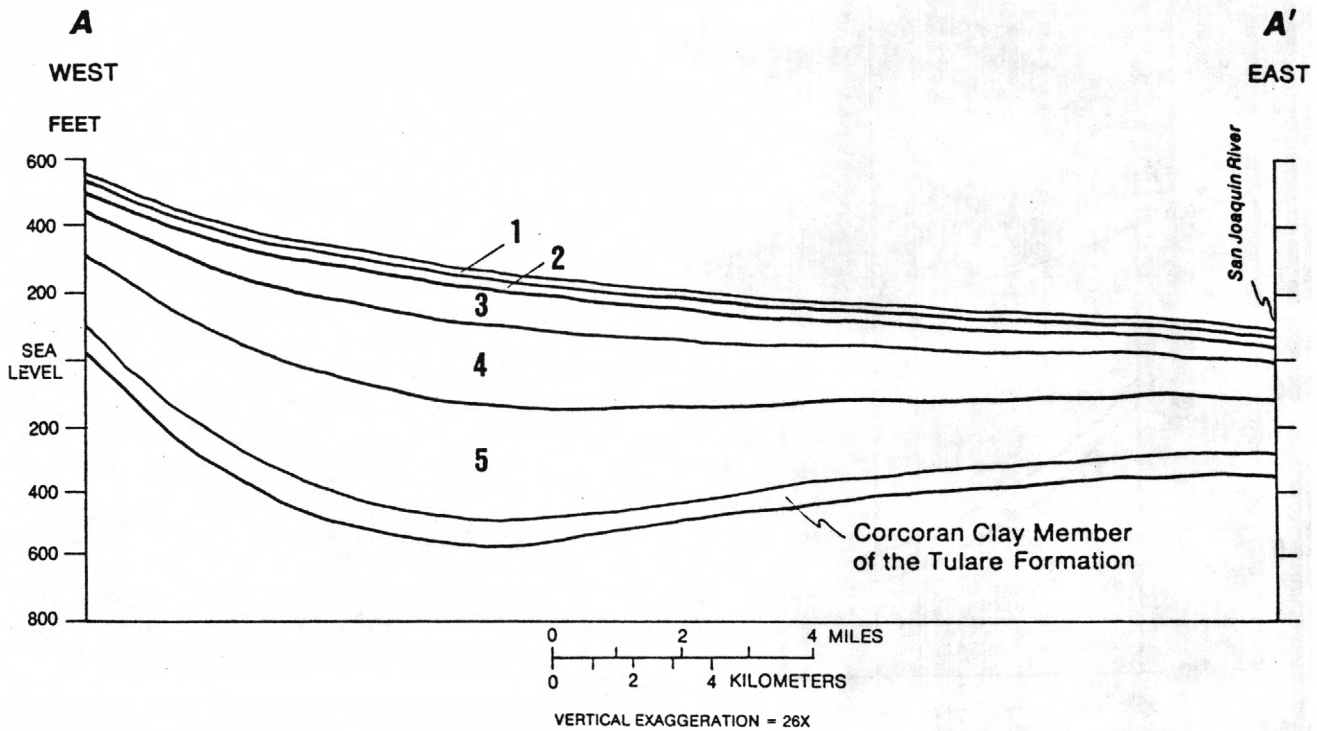

Figure 3. Generalized geohydrologic section of the relative thickness of the five model layers for the semiconfined zone. Layers 1 and 2 are 20 and 30 feet, and layers 3-5 are three-sixteenths, five-sixteenths, and one-half of the remaining thickness between the bottom of layer 2 and the top of the Corcoran Clay Member. Thickness of Corcoran is not to scale.

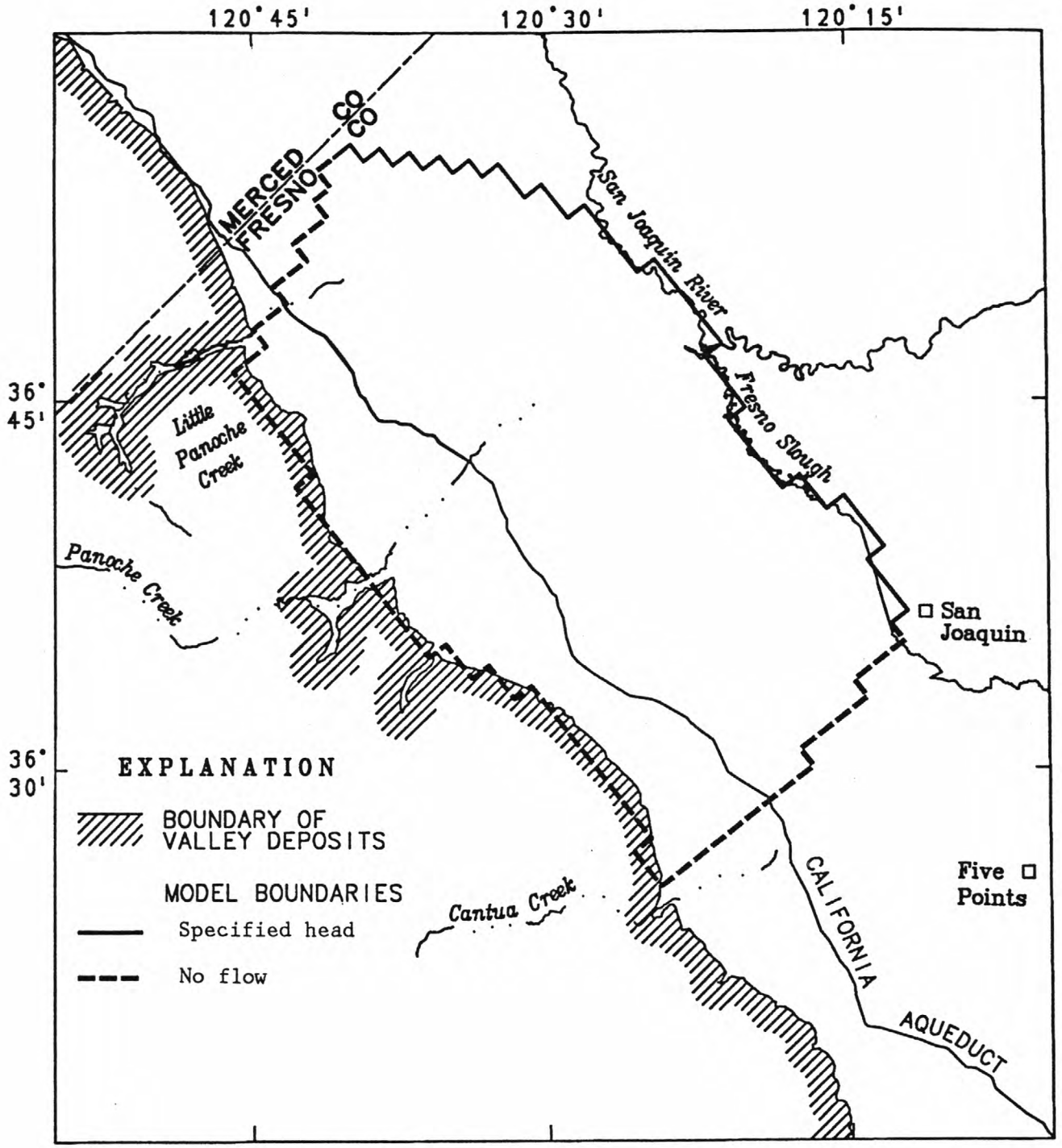

Figure 4.—Lateral boundary conditions.

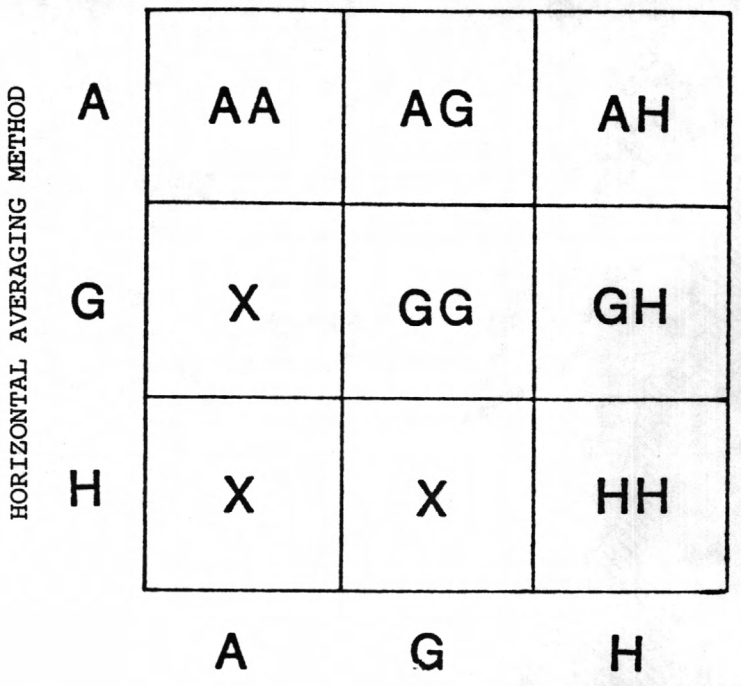

Figure 5. Six possible combinations of horizontal and vertical averaging methods assuming that the horizontal hydraulic conductivity is always greater than or equal to the vertical hydraulic conductivity.

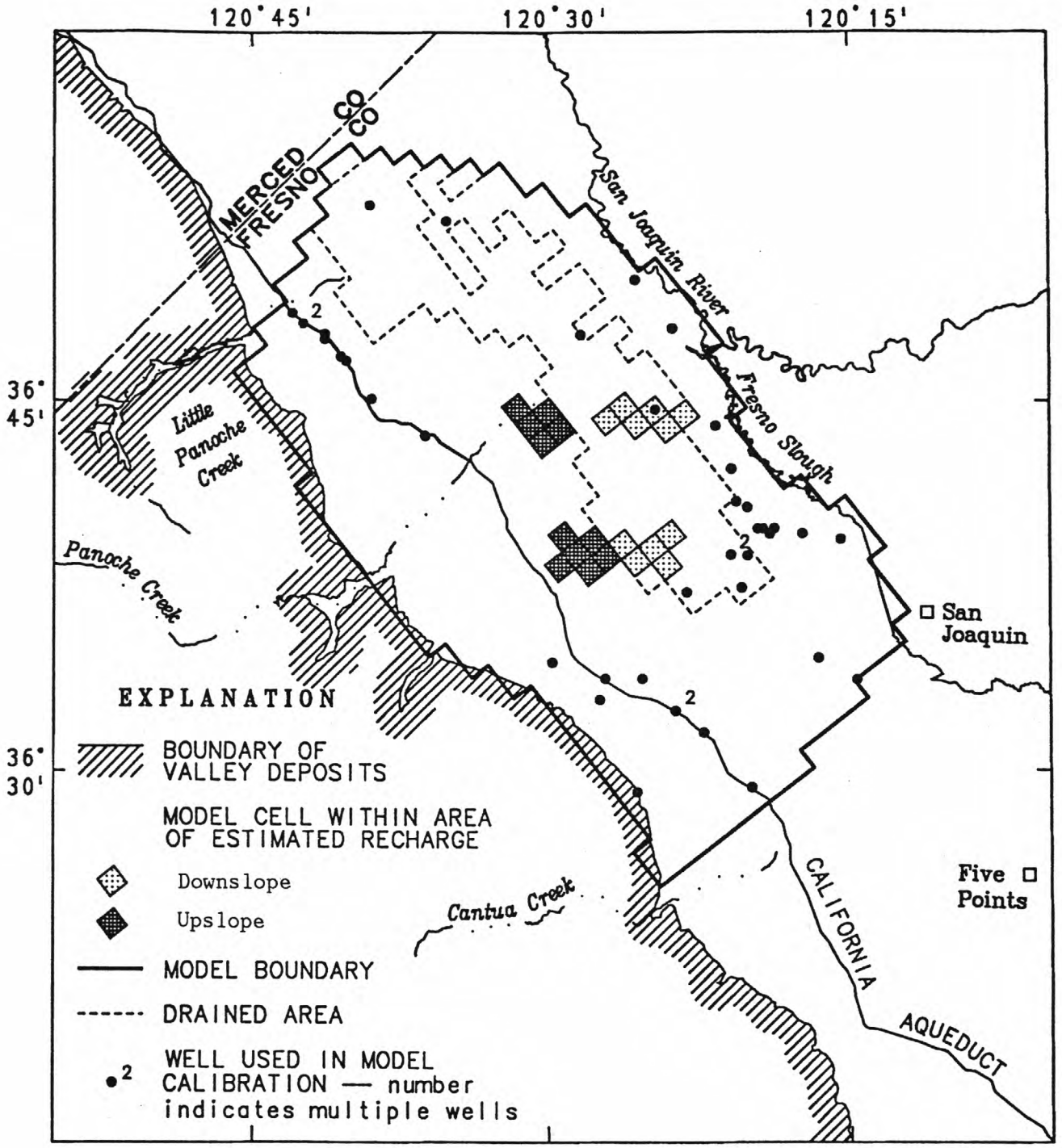

Figure 6. Locations of wells used in head calibration and areas used in flux calibration.

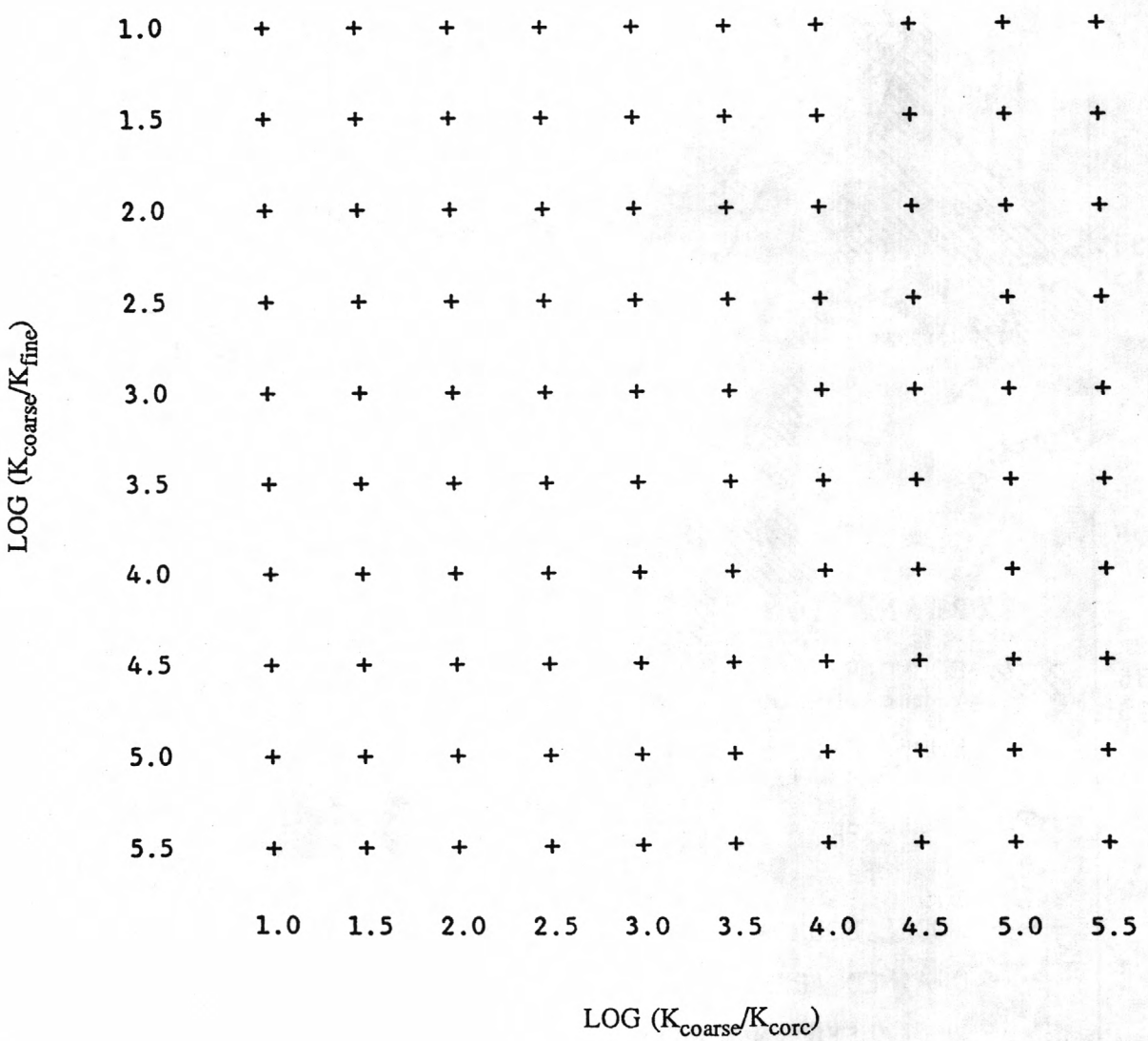

Figure 7. Example of map used to show results from 100 simulations over a range of hydraulic conductivity end members. Each "+" sign represents the results from a single model run using the end member K values indicated on the axes, and a specified combination of horizontal and vertical averaging methods.

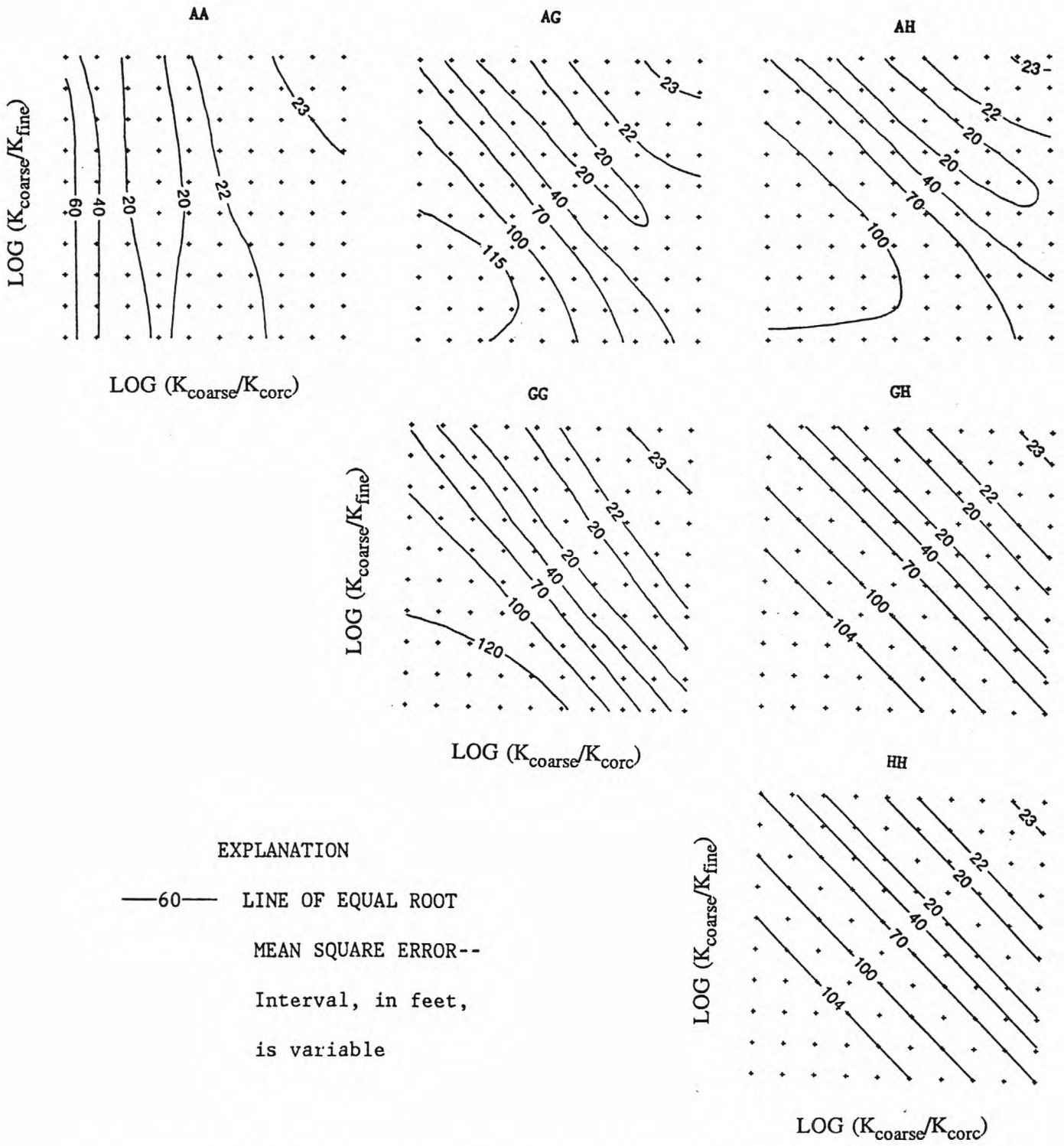

Figure 8a. Root mean square error maps for all six combinations of horizontal and vertical averaging techniques for 1984. For detailed explanation of axes, see Figure 7.

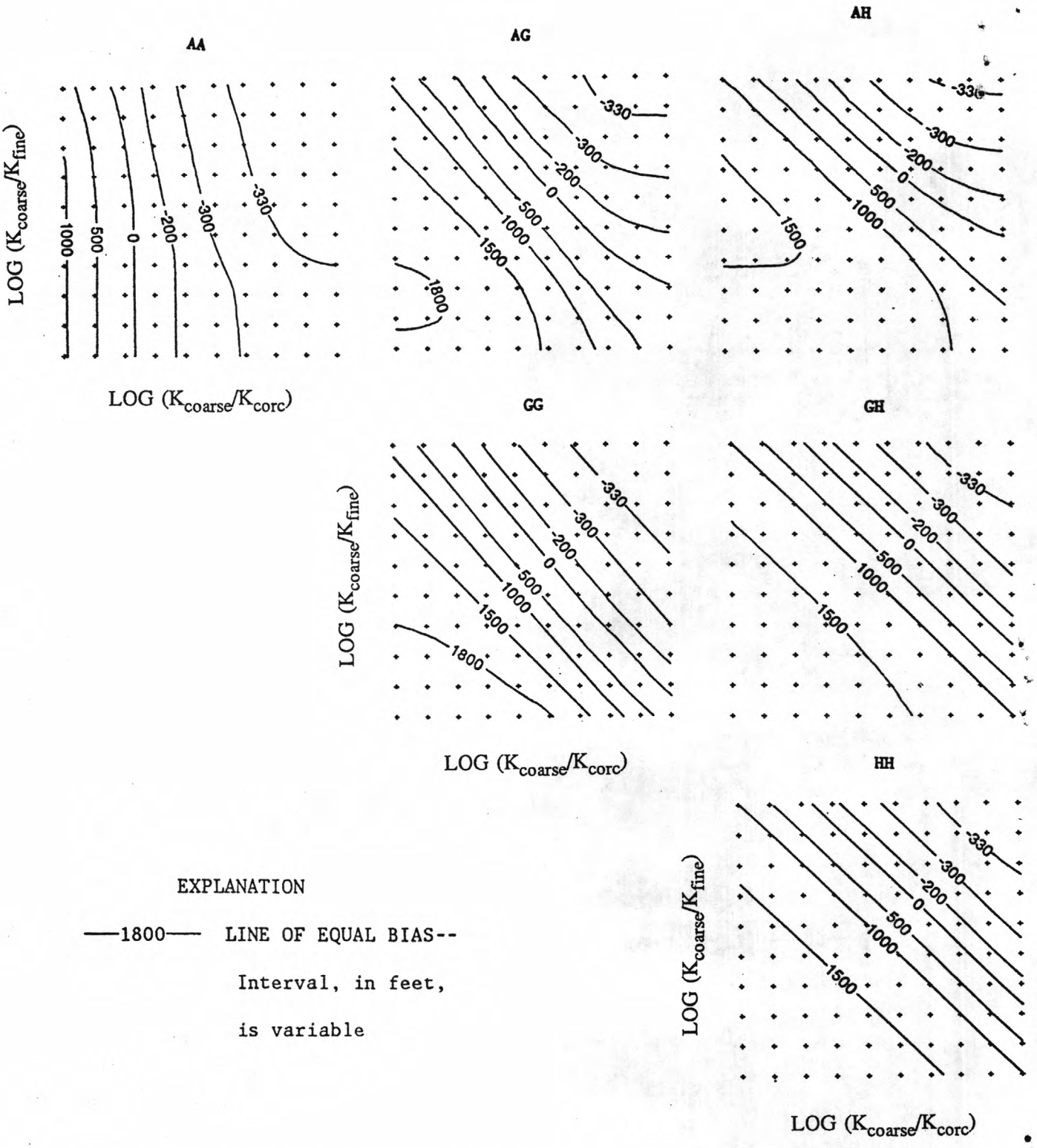

Figure 8b. Bias maps for all six combinations of horizontal and vertical averaging techniques for 1984. For detailed explanation of axes, see Figure 7.

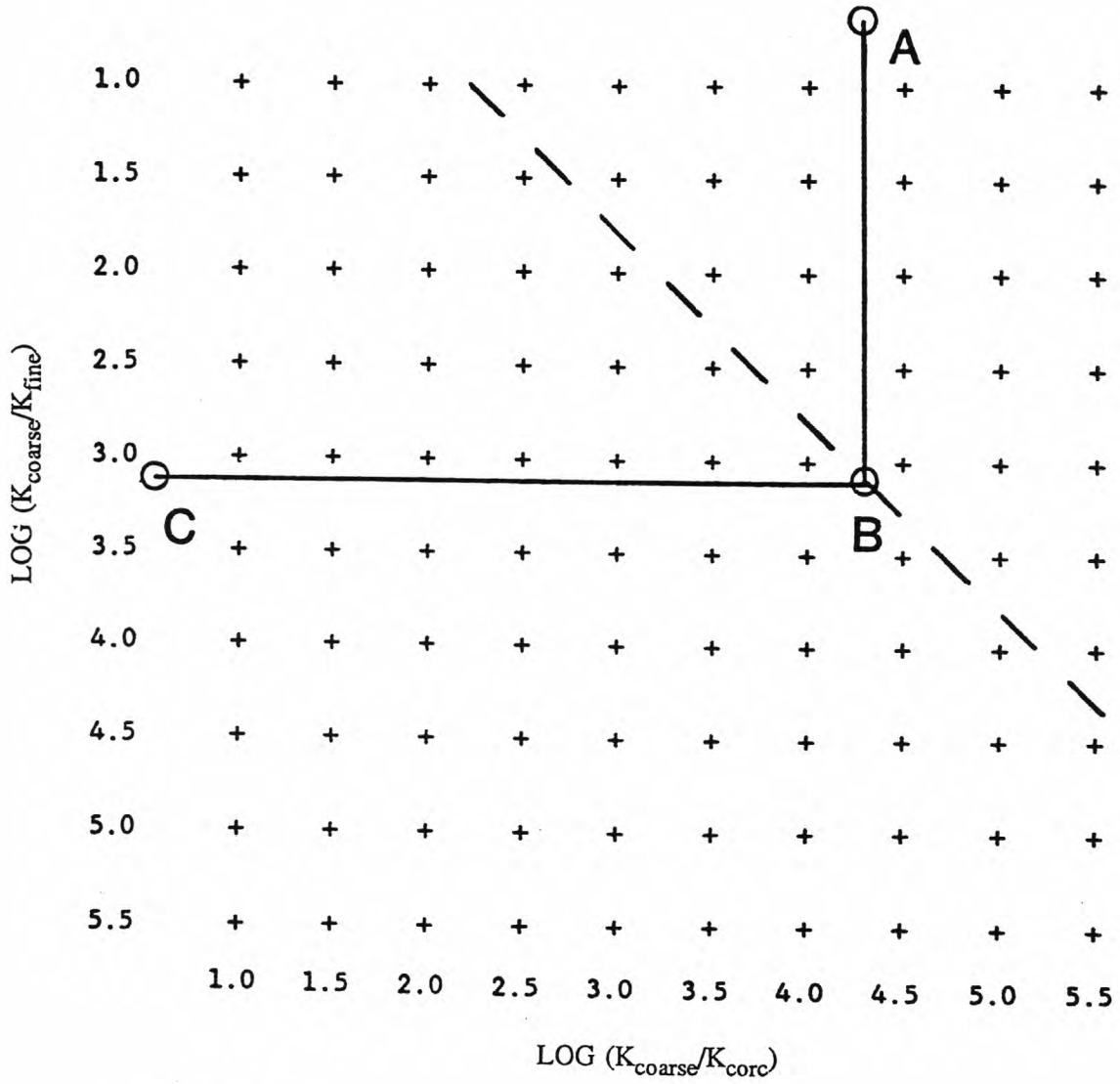

Figure 9. Procedure for determining the optimum K_{fine} when given K_{corc} and K_{coarse}. First, the location of point A is determined by taking the log of K_{coarse}/K_{corc}. Second, a vertical line is dropped from point A until it intersects with the line of minimum root mean square error (point B). Point C is defined by the intersection of a horizontal line between point B and the K_{coarse}/K_{fine} axis. K_{fine} then is determined mathematically given the K_{coarse}/K_{fine} ratio at point C.

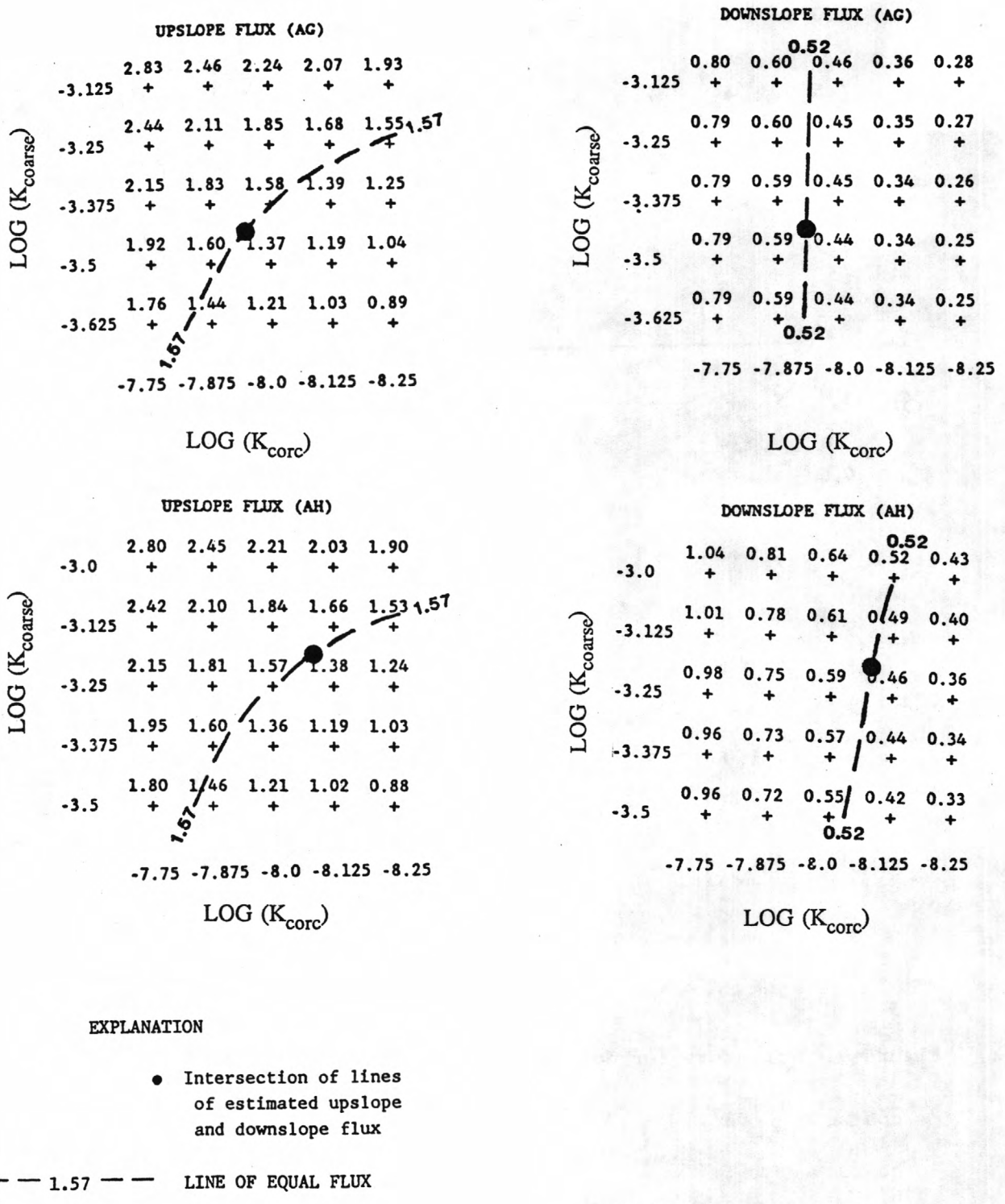

Figure 10. Flux results in one-eight order of magnitude grids. The intersection of the estimated upslope and downslope flux contours represent the optimum solutions for the AG and AH cases.

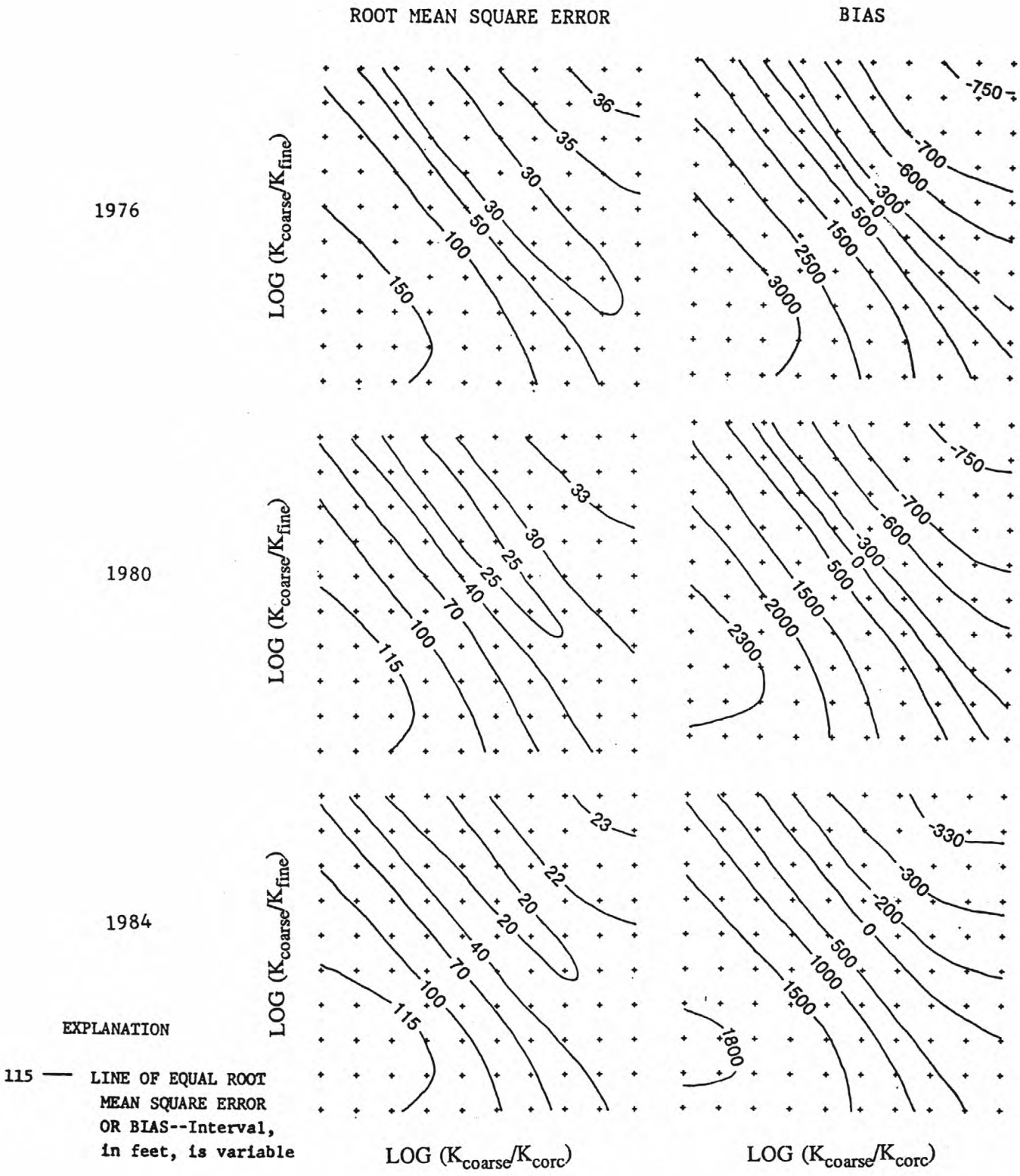

Figure 11. Root mean square error and bias for the AG combination of horizontal and vertical averaging techniques, 1976, 1980, and 1984. For detailed explanation of axes, see Figure 7.

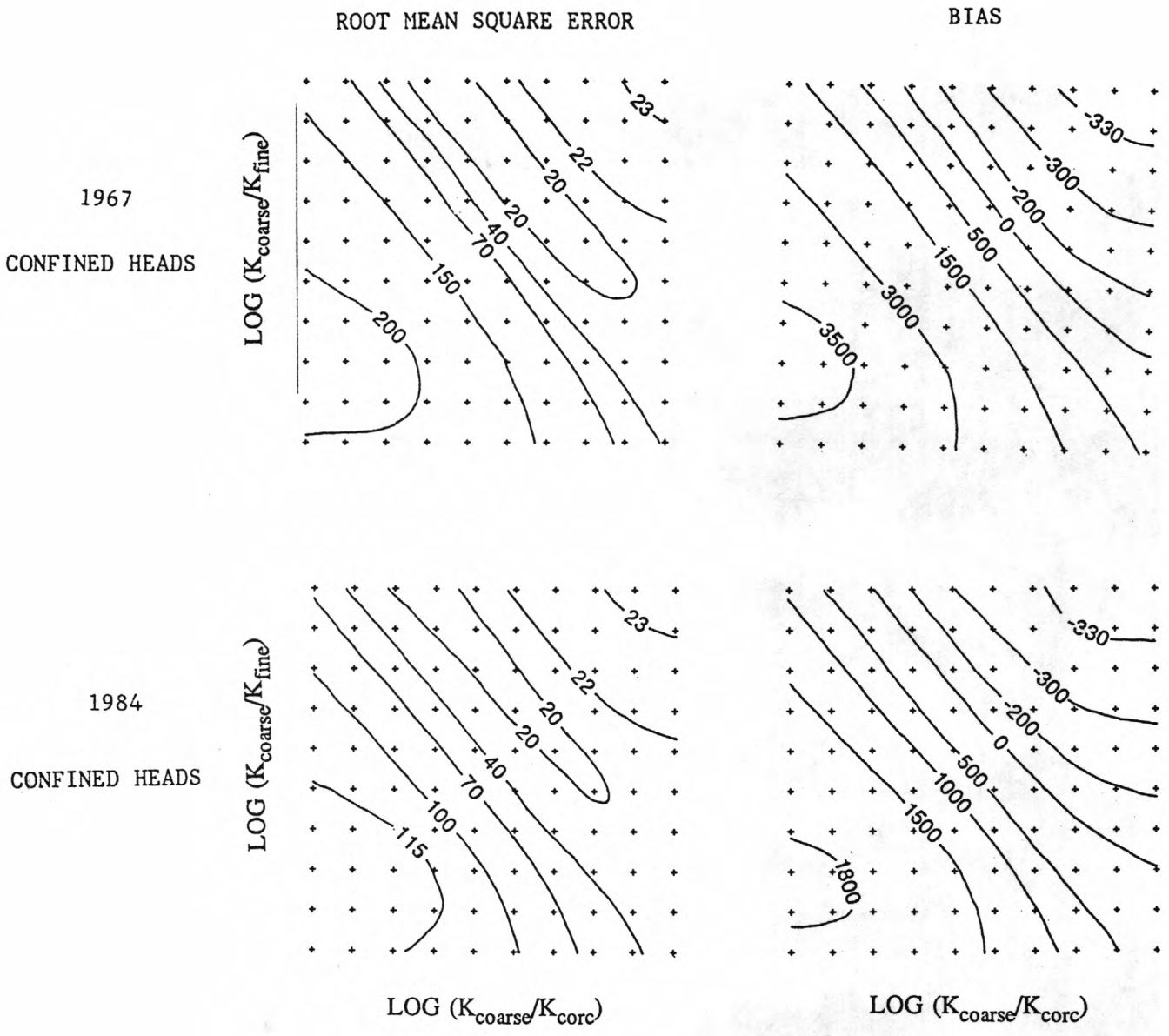

Figure 12. Root mean square error and bias maps for the AG combination of horizontal and vertical averaging techniques, 1984. The upper two maps were created by substituting 1967 values for the confined heads. For detailed explanation of axes, see Figure 7.

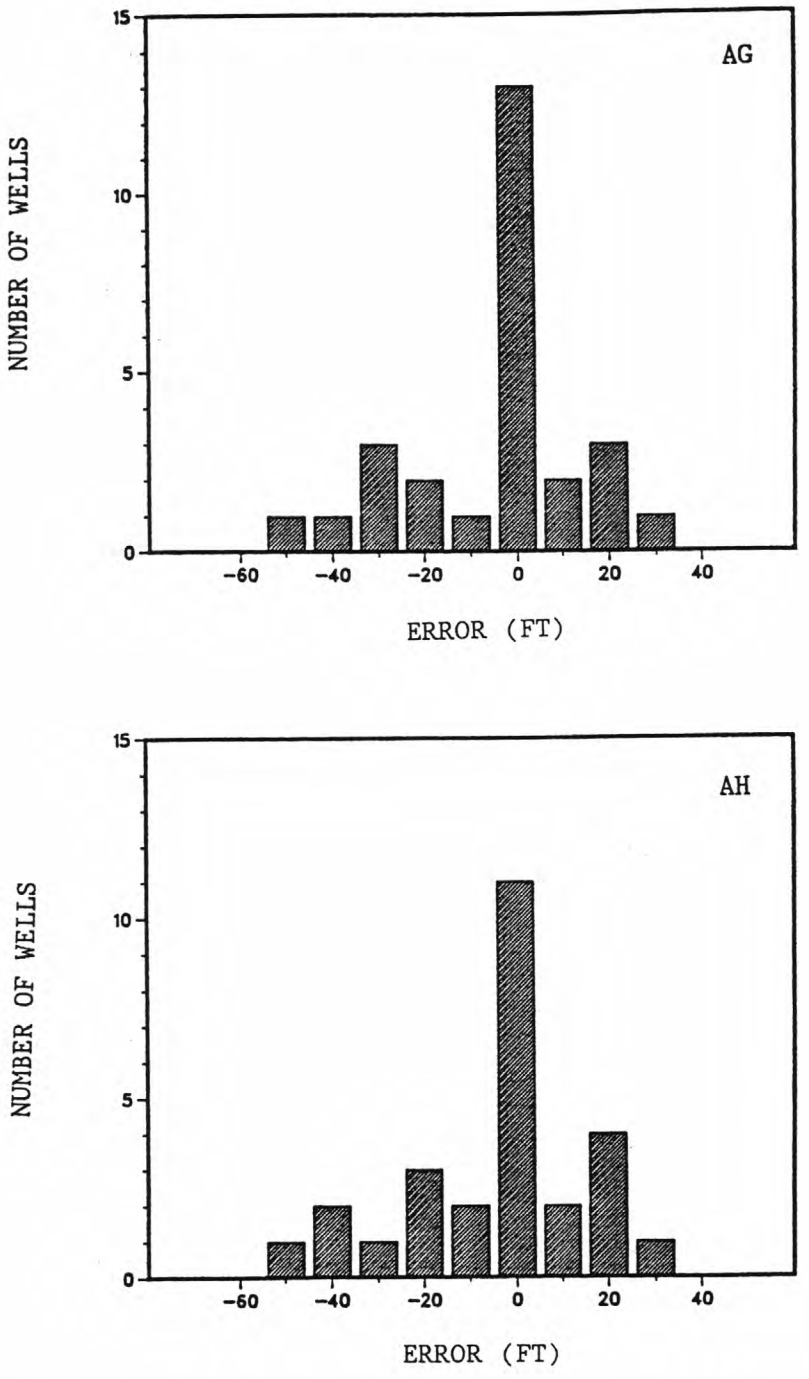

Figure 13. Error between simulated and measured heads for the AG and AH combinations of horizontal and vertical averaging techniques.

Table 1. Slug test results for 25 wells screened in sand

	Number of wells	Hydraulic conductivity (ft/s)	
		Mean	Median
Coast Range sand	17	3.6×10^{-4}	1.4×10^{-4}
Sierran sand	8	1.2×10^{-3}	8.8×10^{-4}
Total	25	6.3×10^{-4}	4.2×10^{-4}

Table 2. Summary of laboratory-determined hydraulic conductivity results for various materials from in and around the study area (modified from Johnson et al., 1968)

Material	Vertical hydraulic conductivity (ft/s)		Horizontal hydraulic conductivity (ft/s)	
	Mean	Median	Mean	Median
Sand	8.6×10^{-5}	2.1×10^{-5}	1.4×10^{-4}	8.2×10^{-5}
Silty sand	1.9×10^{-6}	2.4×10^{-7}	7.6×10^{-6}	6.6×10^{-7}
Sandy silt	9.7×10^{-7}	3.9×10^{-7}	1.0×10^{-6}	4.6×10^{-7}
Sandy silty clay	3.8×10^{-8}	1.4×10^{-8}	7.0×10^{-8}	7.0×10^{-8}
Clayey silt	5.8×10^{-9}	3.1×10^{-9}	6.6×10^{-9}	6.2×10^{-9}
Silty clay	3.1×10^{-9}	1.5×10^{-9}	9.7×10^{-9}	6.2×10^{-9}

POSTAGE AND FEES PAID
U.S. DEPARTMENT OF THE INTERIOR
INT 413

U.S. DEPARTMENT OF THE INTERIOR
Geological Survey
345 Middlefield Road MS 435
Menlo Park, CA 94025

OFFICIAL BUSINESS
PENALTY FOR PRIVATE USE $300
SPECIAL 4TH CLASS BOOK RATE

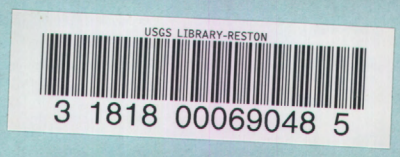

Phillips and Belitz--CALIBRATION OF A TEXTURE-BASED MODEL OF A GROUND-WATER FLOW SYSTEM, WESTERN SAN JOAQUIN VALLEY--OFR 90-573